JLAB-TN-06-014
Yu-Chiu Chao

Testing Rationale of 12 GeV Globally Optimized Optics in 6 GeV CEBAF

Background

The global 5.5 pass lattice solution for the 12 GeV optics contains a major deviation from that currently implemented for the 6 GeV CEBAF, in that a global optimization has been carried out to minimize the highest X & Y β-functions at any point in the entire machine, and to trade off between lower and higher passes such that the β-functions at higher passes, where effects due to synchrotron radiation (SR) induced emittance growth is most significant, are reduced at an expense to the β-functions at lower passes. The need for such optimization is more acute for 12 GeV than for 6 GeV, both because of stronger SR emittance growth at higher energy as mentioned, and because of higher entry momentum ratio between the lowest and highest passes at 12 GeV, due to different momentum profile and an additional pass in the North Linac, which would force the higher pass β-functions to increase considerably if such optimization were not carried out. Study shows that this optimization resulted in reduction of peak β-functions in the last passes from above 400 m in a scheme akin to the 6 GeV lattice[1], to less than 300 m in the globally optimized scheme. This is mainly achieved by reversing polarities of the two quadrupoles shared by all higher passes (i.e., above first pass) at the entrance to the North Linac, reinforcing the initial focusing in both planes for all higher passes except the second, where the beam profiles experience over-focusing and become larger. For detail of the method of optimization see [1].

Due to its deviation from the optics scheme proven through 6 GeV CEBAF operation, the 2005 Lehman Review panel recommended as action item a beam based test of this new rationale applied to the 6 GeV CEBAF. Although the momentum ratio between passes and the level of synchrotron radiation induced emittance growth typical of 6 GeV CEBAF are not such that great benefit can be gained by going to this optimized optics, successful running under this scheme in a real beam based environment would nonetheless go a long way toward confirming its viability. Any problem encountered in such a test would also provide valuable guidance to design and operation with this optics for 12 GeV.

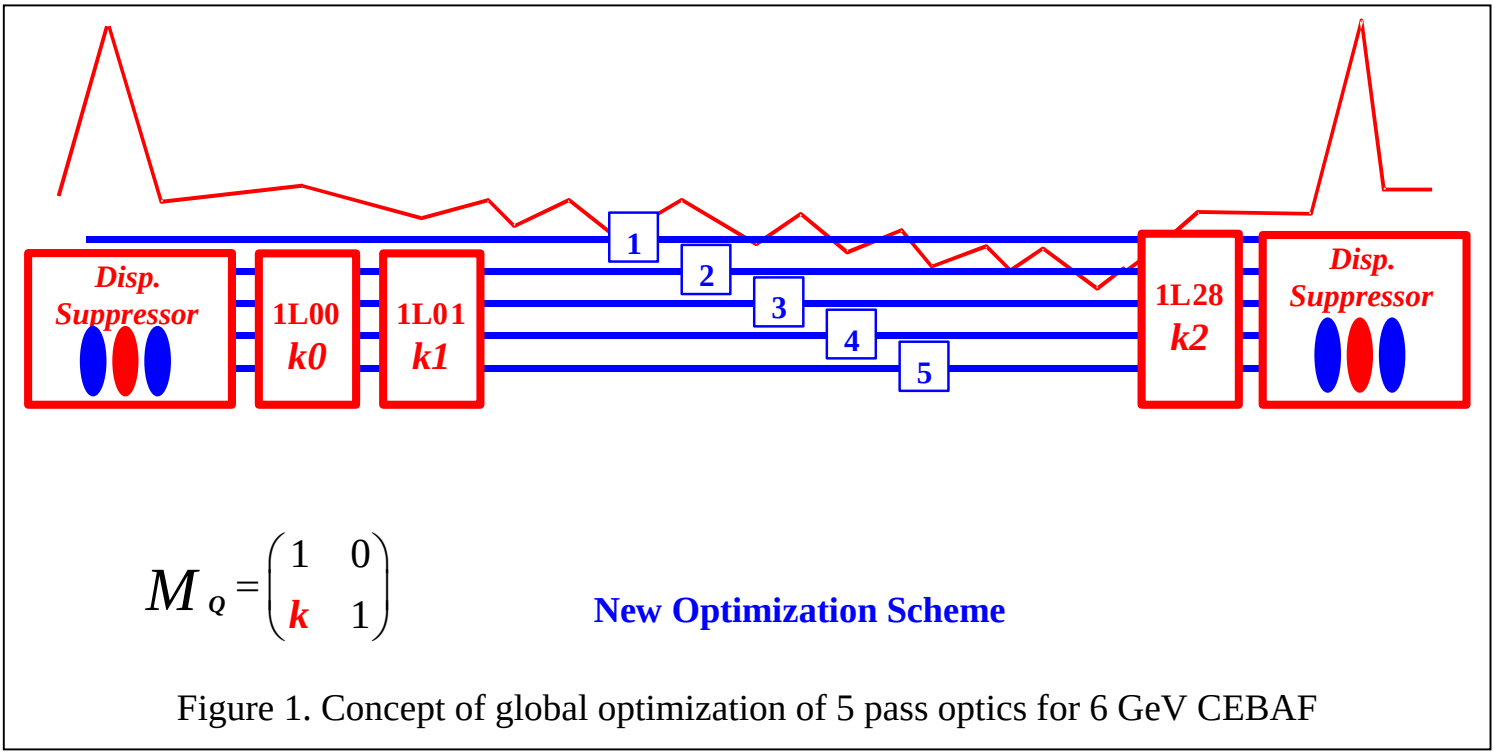

Figure 1. Concept of global optimization of 5 pass optics for 6 GeV CEBAF

Design Optimization

To achieve this goal, the machine configuration, including linac momentum profile and Spreader/Recombiner layout used for the 12 GeV optimization [1] must be replaced by that for 6 GeV CEBAF, before the same analysis is performed. This was done by extracting the running 1.04 GeV/Linac[2] parameters of December 2005 from the accelerator database, and the current CEBAF Spreader/Recombiner geometry and optics from the online model server. The same analysis as that described in [1], with the exception of one less recirculation in the North Linac, was carried out. Figure 1 shows the concept of this process. A two dimensional scan of the strengths[3], k0 and k1, of the two quads 1L00 and 1L01 common to passes 2 to 5 was done, with optimization performed at each scanned point over entry and exit Twiss parameters to achieve smallest global beam profile. The region under study contains the two dispersion suppressors at both ends of each pass for reasons elaborated in [1].

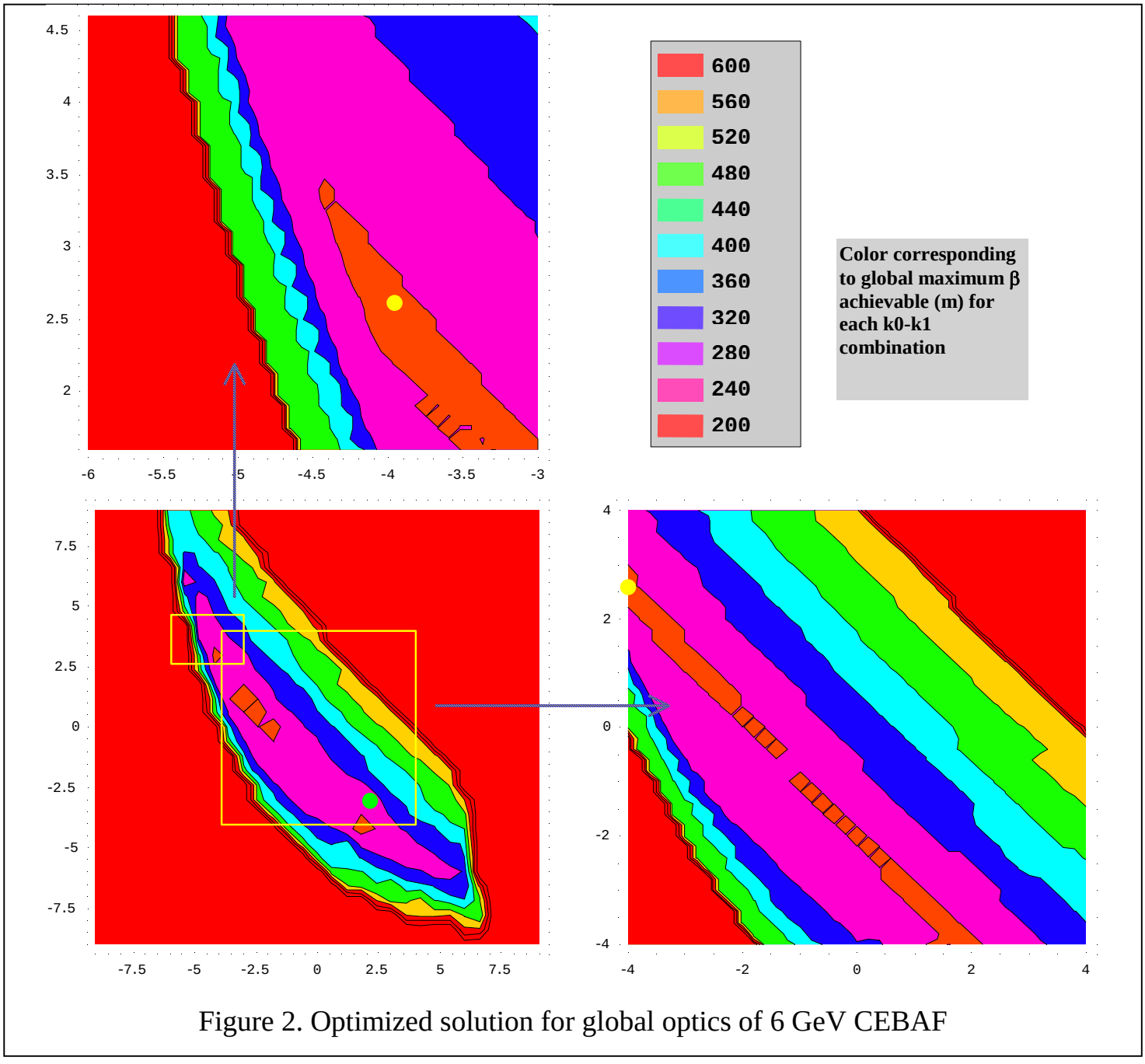

Figure 2. Optimized solution for global optics of 6 GeV CEBAF

---

[1] This assumes the baseline 12 GeV North Linac momentum profile, with all high gradient cryo-modules at the end. For the scheme where all high gradient cryo-modules are at the beginning, the peak β for global optics close to the 6 GeV paradigm is around 360 m.
[2] Rigorously, the 5 pass energy at which this test was done was 5.26 GeV rather than 6 GeV.
[3] Expressed in terms of M_{12} of the quad transfer matrix in m^{-1}.

Figure 2 summarizes the two dimensional scan of the quad strengths. The parameter space spanned by these two strengths k0 and k1, each running from –7.5 m^{-1} to +7.5 m^{-1}, is shown in the lower left corner. Areas in yellow boxes are zoomed in and shown in adjacent plots for detail. The color values at a given point point, indicated by legends in the upper right corner, represent the smallest global (all passes, both planes, Spreader/Recombiner included) β in meters that can be achieved for the combination of k0 & k1 for that point. The yellow dot shown in the close-up plots, centered inside the island of 200 m maximum β functions, corresponds to the solution for k0 and k1 chosen for the optimized solution. Incidentally the green dot corresponds to the k0 and k1 for the current 6 GeV design. This does not however imply that the current design has a maximum β near 240 m indicated by the color code, as it has not been subjected to the same optimization procedure as employed in this analysis. The current design optics has a peak β around 270 m in the 5th pass.

As with the 12 GeV study [1], it is worth noting that some variation to the single pass optics in the North Linac can enhance the solution space for low β functions. Figure 3 shows two such examples: reducing the strength of the 1L28 quad by half, and using a 150° per cell optics in North Linac.

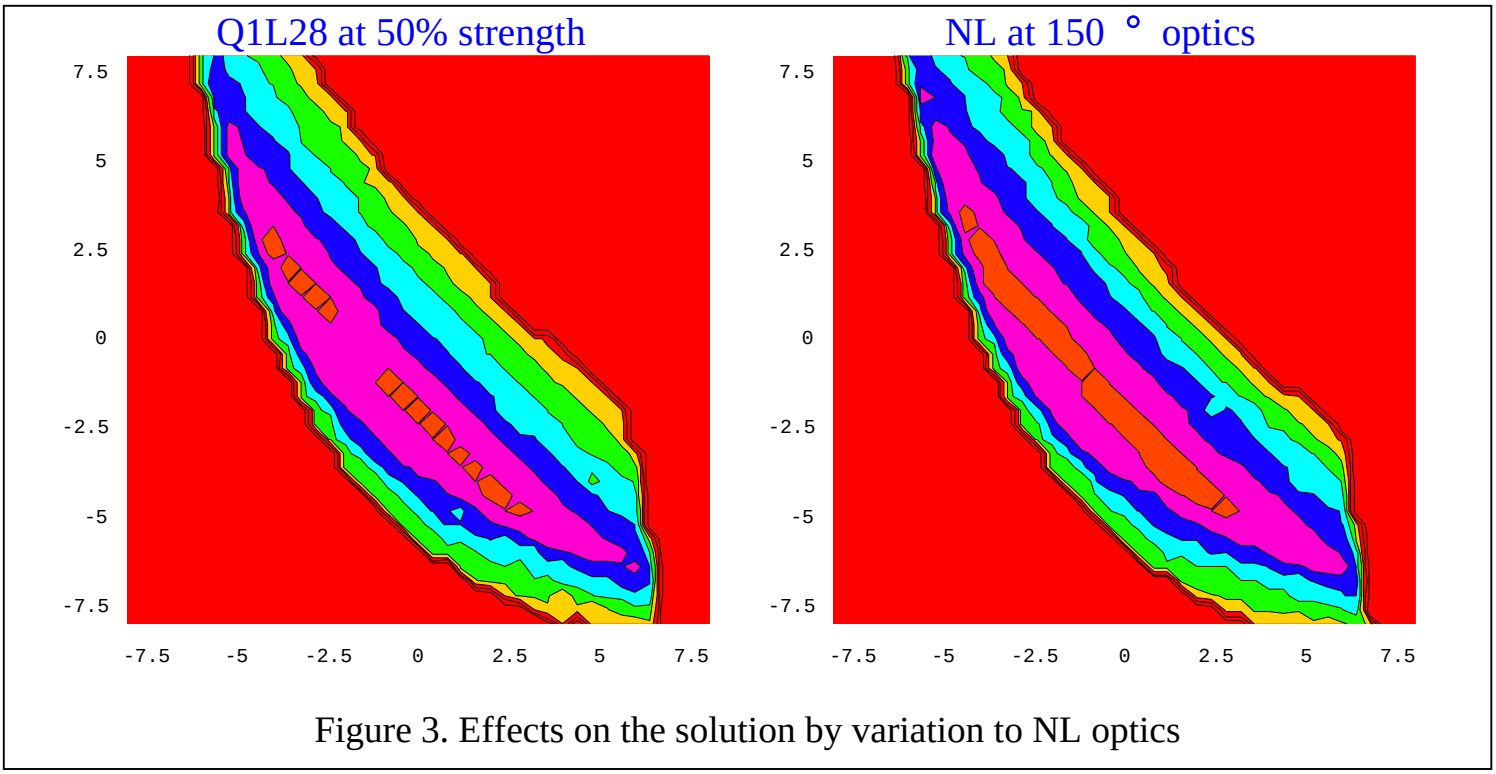

Figure 3. Effects on the solution by variation to NL optics

Following the selection of optimal k0 & k1, the optimal entry and exit Twiss parameters for each pass and each plane are uniquely defined. It remains to match these Twiss parameters to upstream Recombiners and downstream Spreaders using standard matching quads in these regions[4]. Figure 4 shows the contrast between the baseline and the optimized 12 GeV style optics for the 4 highest pass (pass 2 to 5) in the NW Recombiner, North Linac, and NE Spreaders. Indeed the global maximum β function is about 210 m, which is made possible by the considerably over-focused second pass causing the β function there to be near the global maximum. This is in adherence to the philosophy of the 12 GeV optics, namely, trading off between lower- pass and higher-pass beam envelopes through polarity reversal of the reinjection quads, marking a deviation from the standard 6 GeV optics[5].

[4] The dispersion suppressing quads in the actual 5.26 GeV CEBAF were seen to deviate from design values in some passes. We decided to respect these values obtained through beam based tuning and regard all Spreaders and Recombiners as already dispersion suppressed before downloading the betatrom matching quads. Any dispersion leakage, however, will be addressed following standard procedure after this download.

[5] The contrast between the baseline scheme and the 12 GeV schemes in the 6 GeV CEBAF is not as pronounced as that for the 12 GeV 5.5 pass machine, due to much smaller lowest-to-highest pass momentum ratio for the first few zones.

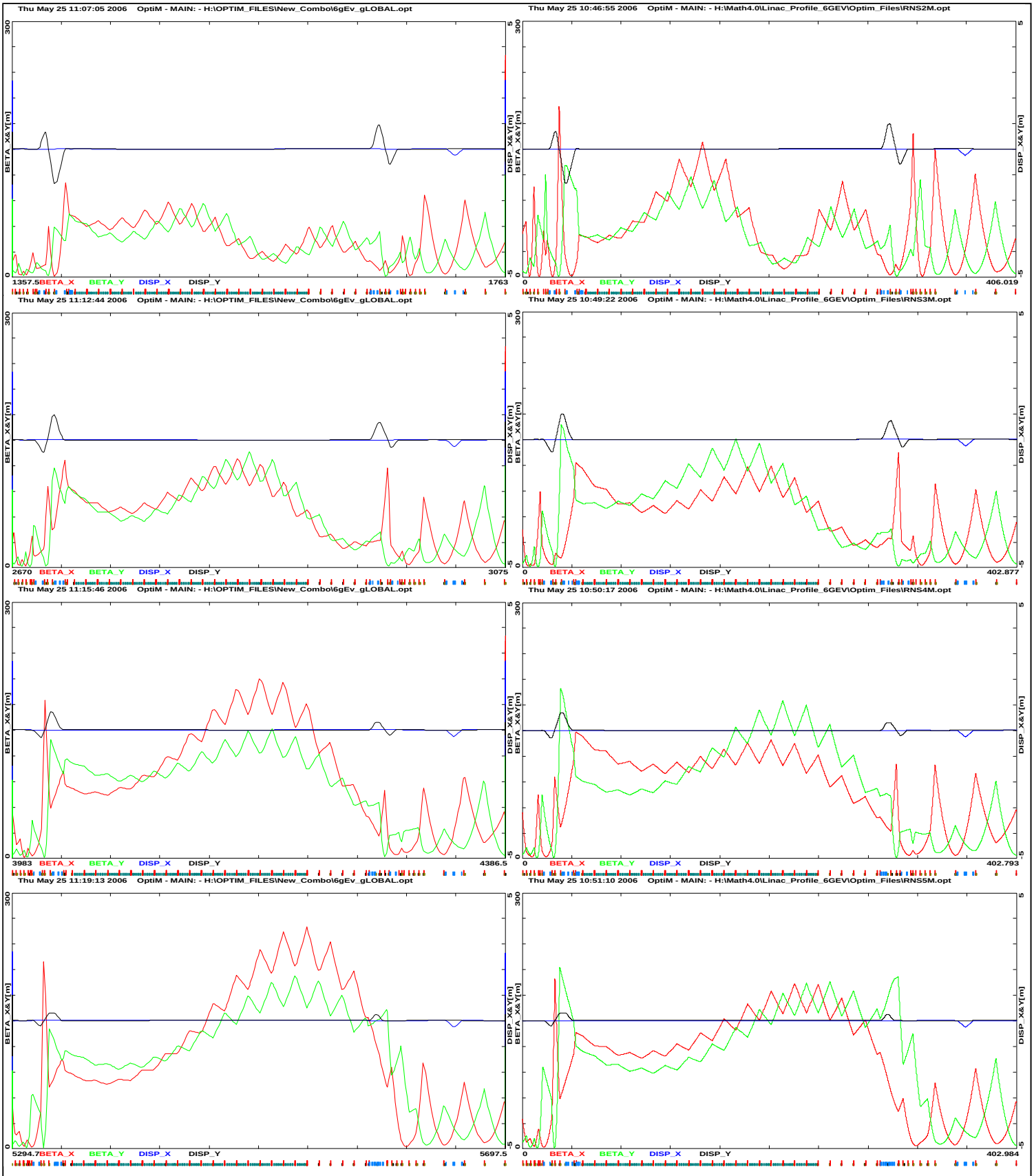

Figure 4. Pass 2-5 Matched Twiss Parameters (Vertical range: 0-250 m)
Left plots: Baseline 6 GeV; Right plots: 12 GeV style optics.
Contrast not as pronounced as in the 12 GeV machine, due to much smaller lowest-to-highest pass momentum ratio for initial NL zones

Implementation

A test plan was submitted to implement this new optics into the 6 GeV CEBAF. As mentioned, this mainly involved changing the focusing pattern at quads 1L00 and 1L01, followed by re-matching the newly optimized Twiss parameters to all upstream Recombiners and downstream Spreaders. The matching quad solution obtained offline would serve as a starting point, with any residual mismatch corrected by empirical online procedure[6]. The contrast between existing and new matching quad values, as well as those for 1L00 and 1L01 quads, are given in **Appendix One**.

This test was carried out during the December 2005 Machine Development period. The quad changes were implemented pass-by-pass, followed by the entire suite of 5 pass machine setup and finalization procedures, known as ORFP. No obstacle was encountered during the setup, and the machine was left in this state for the following several days[7]. Empirical tuning after the initial download resulted in modest changes to the betatron matching quads, most of which needed to change by less than 10% from the design values. The only exception was a 23% change to one matching quad in Recombiner 5, which is not grossly exceptional for ordinary CEBAF tuning. Thus claim of ability to predictably implement such an optics from first principles is quite defensible[8]. Apart from interruptions due to unrelated hardware problems, this new optics has resulted in uneventful 5 pass beam transport, whenever scheduled, during these days.

Analysis of Data

There are several aspects to the conclusion that can be drawn from data acquired during this test.

Beam Profile Measurement

Beam profile measurements were carried out before and after this implementation, using a "quad-scan" procedure in the experimental Hall B running 5 pass beam. The results (ELOG 1302327 for baseline optics, and ELOG 1321986 for 12 GeV optics) showed basically unchanged X & Y emittances (see Table 1). Beam profiles (Twiss parameters) at 5 pass in Hall B were different for the two cases before any attempt at beam profile matching, which was not surprising[9]. Basically beam profile measurements, performed as a standard beam characterizing procedure, did not point to adverse consequence of the 12 GeV optics.

	X			Y		
	ε (nm-rad)	β (m)	α	ε (nm-rad)	β (m)	α
Baseline	0.195±0.025	141.56±29.4	3.262±0.692	0.115±0.008	77.97±10.7	0.758±0.196
12 GeV	0.158±0.006	137.4±4.10	3.370±0.091	0.097±0.025	167.8±37.1	-0.298±0.288

Table 1. Emittance & Twiss Parameters Measured for 5 Pass Hall B Beam under Baseline and 12 GeV Style Optics

Optical Stability Derived from Lock Corrector Distribution

A primary motivation for the new 12 GeV optimized optics was to reduce the optical sensitivity at higher passes through reduced β functions there. Similar benefit is expected in the optimized optics for 6 GeV. Thus any

[6] As the standard transport matching tool used at CEBAF, the 30 hz Courant Snyder plots, has as its objective mapping the design Twiss parameters from one Arc to the design Twiss parameters to the next, and because the Arc design Twiss parameters never change, this remaining matching can be done directly with the 30 hz Courant Snyder tool without the need to update the design model to reflect the new optics.

[7] Roughly from December 16 to December 23. Five pass beam was not delivered throughout this period. The total time of 5-pass beam delivery under this optics amounted to several shifts.

[8] For detail of tuning changes see ELOGs: 1302541, 1302317.

[9] The standard Courant-Snyder transport matching from Arc 1 to Arc 9 was nonetheless done in both cases, possibly explaining the closeness of the measured Twiss parameters.

beam based evidence of lower optical sensitivity, manifested through reduced fluctuation in the correctors used in the slow orbit feedback system, or "locks", would indicate this motivation is indeed justified.

The corrector and BPM read-back values can all be retrieved from the accelerator Archiver system. Data from the following periods with 5 pass beam present were recovered for analysis.

Baseline Optics:	2005-12-15:00:00:00 to 2005-12-15:04:00:00
	2005-12-15:20:00:00 to 2005-12-16:07:00:00
12 GeV Optics:	2005-12-22:21:35:00 to 2005-12-22:22:10:00
	2005-12-22:22:15:00 to 2005-12-22:23:50:00
	2005-12-23:00:20:00 to 2005-12-23:02:00:00

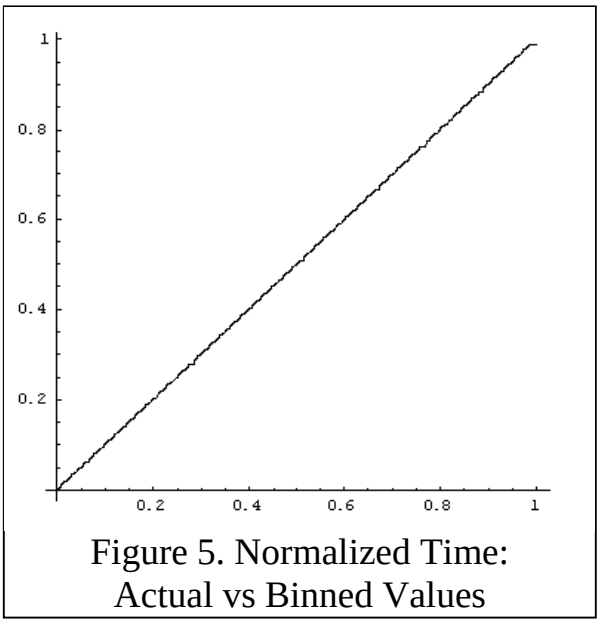

Figure 5. Normalized Time: Actual vs Binned Values

The approach was to obtain, out of this archived data, as many as possible snapshots of the entire machine covering all pertinent corrector and BPM signals[10] logged within a small time window of each other. We could then treat each such snapshot as a quasi-real beam orbit through the machine, and extract a pattern of impact of optical sensitivity on its evolution, which should emerge with sufficiently large ensemble of snapshots in the form of histograms of distributions. This synchronism was achieved by collecting archived data into time bins of 10 seconds. Synchronism between signals proved to be quite decent under this binning scheme, as demonstrated in Figure 5, showing correlation between two time representations of all logged read-backs of a BPM: the real event time and the bin time it falls within. Both times are normalized to make the total archived period equal to one. It can be seen that the binning process caused minimal distortion to the real event time, thanks to pretty dense archiving.

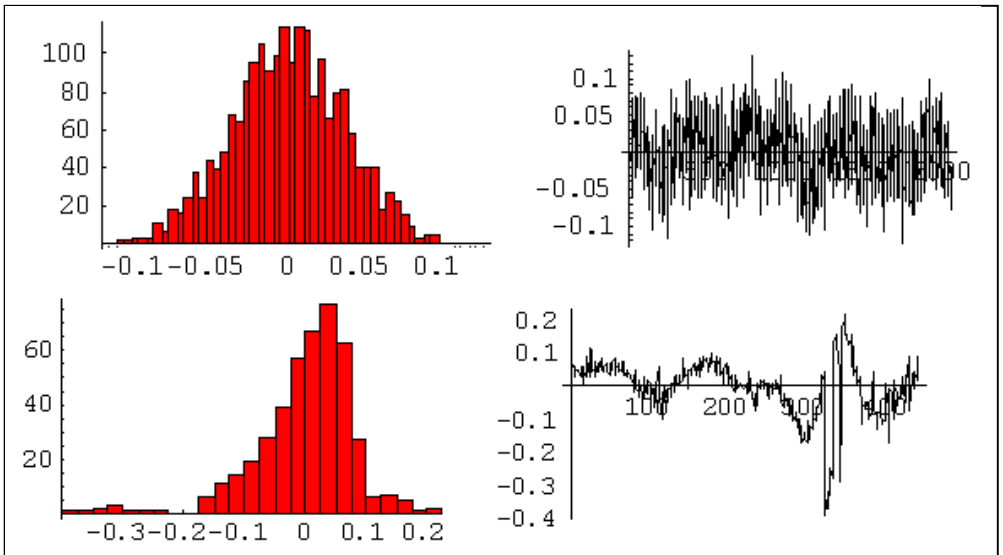

Figure 6. Spread of BPM 9S06 Signals before Filtering
Top: Baseline Optics; Bottom: 12 GeV Optics

Another technique necessary for extracting the underlying pattern of sensitivity was a software high pass filter applied to the data. As slower drifts on the order of minutes, which can contribute spuriously to the widths of histograms, are seen to display less long-range correlation and thus less likely representative of variations in optical sensitivity from one region to the next, this filtering ensures that only symptoms attributable to optical sensitivity are included in the histograms. Figure 6 demonstrates the necessity for this filtering. The apparent width of the 9S06 BPM spread for the 12 GeV optics was exaggerated by the slow jumps and drifts that were more likely attributable to changes in beam or operational conditions, making the distribution appear wider than that for the baseline optics. After high pass filtering the two cases presented quite similar widths of distribution.

[10] This includes all correctors and BPM's used by the locks, as well as those immediately upstream of the locks.

Finally, to correctly interpret the degree of fluctuation of the lock correctors, one cannot ignore the BPM's used as input to the locks. The spreads of both components need be taken together for the complete picture. One can instead subtract the pulse-by-pulse corrector contribution from the BPM's to get distributions of the "pre-correction" orbits. In the current analysis, however, we choose to directly look at the orbits entering each lock before any feedback action. This allows us to bypass altogether the question of what is the optimal combination of lock corrector and BPM data to use for studying their distributions.

In this context we used five BPM's at the entrance to the locks in the second Spreader, where the optics is the same for both baseline and 12 GeV style optics, and the 9th Spreader, where one sees the cumulative effect of all differences between these two optics. Thus the first set of BPM's constitutes a control data set, providing screening on effects not related to differences in sensitivity in higher passes between these two optics[11]. The orbits through these 5 BPM's were fitted to the optical models of the respective Spreaders to produce entrance position and angle to the locks. The RMS of the resulting distribution of fitted positions and angles are then calculated. These are given below (in mm mrad):

		IPM2S05		IPM9S04	
		POS	ANG	POS	ANG
6 GeV	X	0.0751709	0.0140916	0.0362862	0.00289593
	Y	0.0508946	0.0151379	0.0291197	0.00115635
12 GeV	X	0.078564	0.0144446	0.0286357	0.00219288
	Y	0.107112	0.0328567	0.0563845	0.00154324

Clearly the machine front end has been intrinsically less stable for unrelated reasons while 12 GeV optics was in place. Since the numbers in Spreader 2 can serve as controls, one can used them to "normalize" the numbers in Spreader 9 for these two optics. This following figure-of-merit normalized numbers are produced, by first dividing the position (angle) in Spreader 9 for each optics by the position (angle) in Spreader 2 for the same optics, then scaling the outcome for 12 GeV optics by that for baseline optics. For example, the "X-position figure of merit" is given by

$$\left(\frac{\langle X^2\rangle_{\text{12 GeV Arc 9}}}{\langle X^2\rangle_{\text{Nominal Arc 9}}}\right) \Big/ \left(\frac{\langle X^2\rangle_{\text{12 GeV Arc 2}}}{\langle X^2\rangle_{\text{Nominal Arc 2}}}\right)$$

This gives the following figure-of-merit table, which provides a measure of the reduction in orbit fluctuation by going from baseline to 12 GeV style optics.

	POS	ANG
X	0.75508	0.738725
Y	0.920039	0.614872

Although not very rigorously constructed, the above numbers do suggest a reduction in orbit sensitivity, independent of front end noises, with the implementation of the 12 GeV optics. We can attempt a more rigorous approach, resorting to the propagation of invariant quantities between Spreader 2 and 9, instead of phase-dependent position and angle, by calculating the fluctuation of Courant Snyder (CS) parameters with respect to design optics at the E02 locations, or extraction points, following these two Spreaders. The reasons for choosing the E02 locations are

- Both optics have to be matched to the same design parameters at 2E02 and 9E02

[11] Such effects can include Injector and North/South Linac fluctuations.

- Unlike in the Spreaders, design Twiss parameters at E02 are physically significant in defining downstream transport quality. They are canonical and constant[12].

Due to effective filtering and synchronization, the fitting to optical models was quite good, and resulting CS distributions display close-to-normal behavior, as shown in Figure 7. This lends credence to our final conclusion on sensitivity. The RMS of the distributions of these calculated CS values are given below. Being single-particle CS parameters, these all have the unit of $m^{1/2}$, up to an arbitrary but uniform scaling factor.

		RMS of CS at IPM2E02	RMS of CS at IPM9E02
6 GeV	X	0.00358569	0.0041759
	Y	0.0154404	0.042744
12 GeV	X	0.00412747	0.00422326
	Y	0.0240341	0.0313307

The same trend is still apparent. Despite larger intrinsic noise from the front end when the 12 GeV style optics was in place, the cumulative noise at 9E02 was smaller with this optics. One can finally try to extend this line of reasoning by normalizing the 9E02 CS by the 2E02 CS, and get for

$$\left(\frac{CS_{\text{12 GeV Arc 9}}}{CS_{\text{Nominal Arc 9}}}\right) \Big/ \left(\frac{CS_{\text{12 GeV Arc 2}}}{CS_{\text{Nominal Arc 2}}}\right)$$

the two numbers, one for each plane, summing up the overall differences between the baseline and 12 GeV optics in terms of optical sensitivity:

X: 0.8786

Y: 0.4709

If one accepts this interpretation, the 12 GeV optics has significantly reduced optical sensitivity, especially in Y. Remember in any case this is deduced from good quality fits to optical models, which in turn came from large distributions (>2000 trajectories × 5 BPM's in each plane) with decent statistical characteristics. Thus despite some caveats inherent in its reasoning[13], the final numbers represent an unmistakable tendency toward lower sensitivity in the 12 GeV optics.

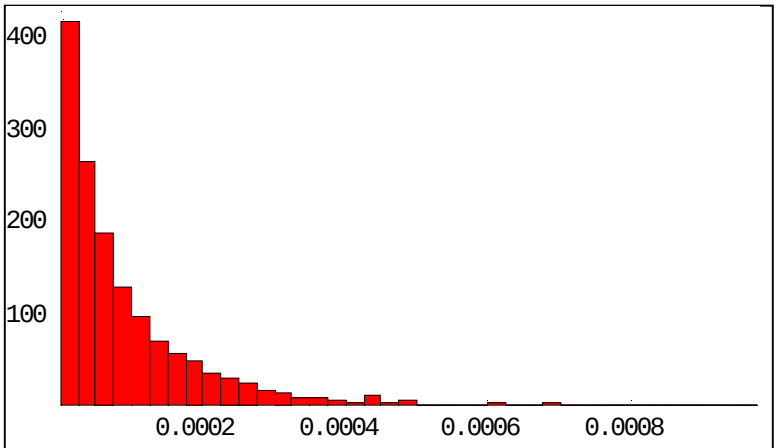

Figure 7. A typical distribution of CS parameters

A test plan with data logging dedicated to comparing orbit stability under these two optics has been submitted, awaiting the next machine development opportunity. This should eliminate some of the uncertainties encountered in the analysis of the current set of data.

[12] We could also use A01 for even better justification, but the result would be the same due to invariance.

[13] Two remaining questions: (A). Whether the real transport between Arc 2 & Arc 9 was consistent with the design Twiss at both ends to allow a direct translation of CS parameters. (B). What states the intervening orbit locks were in during the test. We could not easily answer these 2 questions at this point.

Beam Envelope Evolution Based on Difference Orbits (Raytrace)

During this test an independent study was carried out by Y. Roblin and M. Tiefenback on new methods for acquiring difference orbit data in the machine. It became apparent afterwards that the data collected confirmed important characteristics of the 12 GeV style optics. In these tests difference orbits were generated to mimic in the X-X' or Y-Y' phase space the design beam ellipse at a given point. Once this is done, propagation of this ensemble of difference orbits automatically maps out the empirical β function for the rest of the machine. Figure 8 shows this propagation of difference orbits when the 12 GeV optics was in place. The vertical scale in the top (bottom) plot represents the extent in X (Y) of the orbit ensemble mapped out along the beam line, and is thus an indirect measure of the β-function[14] in X (Y), and it would agree with the design β-function provided the initial ensemble has the same distribution as the design Twiss parameters at that point, or if it is "matched". In the X-plane the initial ensemble was not matched to design Twiss, thus it was not readily visible if the real optics follows the intended 12 GeV style behavior. In the Y plane the initial ensemble was indeed matched to design Twiss, and a close resemblance to the design Twiss in Figure 4 can be discerned, including the level of β at the North Linac entrance (3rd BPM in Figure 8). Unfortunately the beam was stopped before pass 4 when this data wad taken and no conclusion can be drawn for the last two passes.

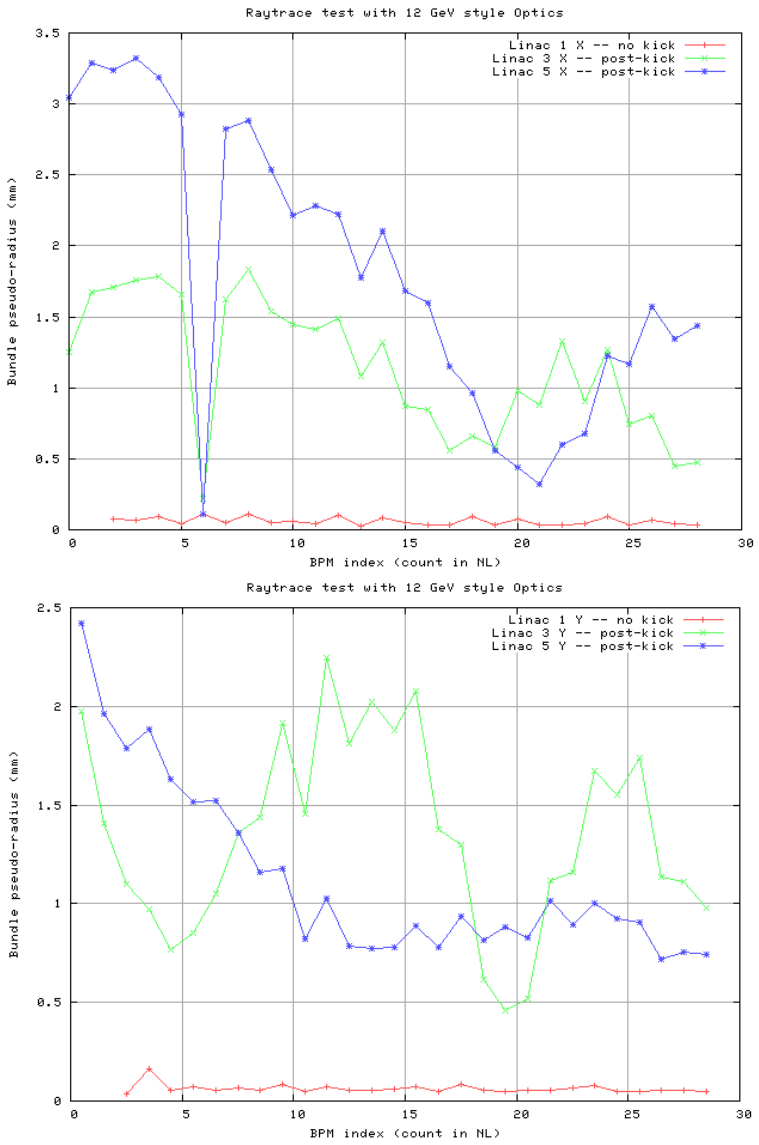

Figure 8. Raytrace Picture Showing Measure of β-Functions for the First 3 Passes in North Linac (Top: X, Bottom: Y; Vertical units are in mm representing extents of orbit distribution in each plane; Horizontal units are in BPM indices. The first 2 BPM's are outside the North Linac.) Courtesy M. Tiefenback

Conclusion

- The global optics design principle for the 12 GeV upgrade was applied to 6 GeV CEBAF, resulting in a new optics involving different operating points for the re-injection quads and corresponding changes to all higher pass matching quads. This amounted to an optimized trade-off between lower and higher pass peak β functions.
- This new optics was implemented during the December 2005 Machine Development period. Standard machine setup procedures were sufficient to bring it online. Stable running with 5-pass beam was reported over a several-day interval (a total of several shifts with 5-pass beam) under this configuration. No impediment to operation due to this new configuration was observed.
- One of the expected benefits of this optics, reduced sensitivity, could be discerned from analysis of archived orbit data showing reduced fluctuation in the presence of the 12

[14] It is however not exactly the RMS of the ensemble, so not exactly β.

GeV style optics. By one reasoning the reduction in RMS width of the distribution of Courant Snyder mismatch parameters was 0.88 in X and 0.47 in Y.

- Other measurements, including beam profile in Hall B and 5-pass difference orbit propagation, confirmed the important characteristics of this optics and further supported its viability.

Appendix One. Quad changes from 6 GeV standard optics to 12 GeV style optics in CEBAF

QUAD	Existing BDL	New BDL	% Change	Maxed out?
Reinjection Quads				
MQB1L00	7557.42	-5117.62	-167.72	No
MQB1L01	-5496.30	7873.26	-243.25	No
Pass 2 Quads				
MQC2A40	1558.02	2408.21	54.57	No
MQC2R01	11735.90	14200.04	21.00	No
MQC2R02	-13837.60	-10201.34	-26.28	No
MQC2R03	22592.50	20054.43	-11.23	No
MQC2R04	-12648.40	-8768.80	-30.67	No
MQC2R05	9897.56	18158.83	83.47	No
MQC2R06	-1067.49	-20092.20	1782.19	No
MQC2R07	-7715.73	15120.17	-295.97	No
MQU3S04	-12075.90	-7329.17	-39.31	No
MQU3S05	17357.80	17050.95	-1.77	No
MQU3S06	0.00	-2700.33	NA	No
MQU3S07	-9246.41	-10447.07	12.99	No
MQU3S08	12011.50	10506.71	-12.53	No
MQU3S09	-11117.50	-8665.55	-22.05	No
MQU3S10	11234.10	10325.10	-8.09	No
MQB3E01	-5916.20	-6471.35	9.38	No
MQB3E02	5424.73	5933.76	9.38	No
MQB3E03	-5485.18	-5999.88	9.38	No
MQU3A01	7374.50	8271.56	12.16	No
Pass 3 Quads				
MQA4R01	26267.20	24003.00	-8.62	No
MQA4R02	-41013.10	-34828.89	-15.08	No
MQA4R03	46804.50	46747.44	-0.12	No
MQA4R04	-46207.00	-44777.49	-3.09	No
MQA4R05	19.53	704.75	3508.72	No
MQA4R06	33374.10	34123.32	2.24	No
MQA4R07	-32951.40	-32157.72	-2.41	No
MQA5S04	-19243.20	-18979.76	-1.37	No
MQA5S05	28529.10	28865.79	1.18	No
MQA5S06	-9555.05	-8864.68	-7.23	No
MQA5S07	-7115.61	-6352.84	-10.72	No
MQA5S08	5441.84	5769.26	6.02	No
MQA5S09	-18525.20	-18638.18	0.61	No
MQA5S10	17879.50	17785.34	-0.53	No
MQB5E01	-8838.56	-8896.54	0.66	No
MQB5E02	9404.38	9526.13	1.29	No
MQB5E03	-8673.13	-8785.41	1.29	No
MQA5A01	12922.00	12897.17	-0.19	No

QUAD	Existing BDL	New BDL	% Change	Maxed out?
Pass 4 Quads				
MQA6R01	27692.70	30843.21	11.38	0
MQA6R02	-37527.60	-35079.72	-6.52	0
MQA6R03	38389.20	40387.98	5.21	0
MQA6R04	-62459.00	-64548.63	3.35	0
MQA6R05	55008.90	49818.45	-9.44	0
MQA6R06	-2481.95	-2773.62	11.75	0
MQA6R07	-35848.50	-35541.57	-0.86	0
MQA7S04	-19373.20	-19609.67	1.22	0
MQA7S05	46935.00	46871.19	-0.14	0
MQA7S06	-17861.70	-17828.02	-0.19	0
MQA7S07	-0.00	247.78	NA	0
MQA7S08	-0.00	405.14	NA	0
MQA7S09	-17914.40	-17408.98	-2.82	0
MQA7S10	21905.60	21560.17	-1.58	0
MQC7E01	-12807.00	-13219.17	3.22	0
MQC7E02	11444.80	11779.85	2.93	0
MQC7E03	-12439.30	-12803.48	2.93	0
MQA7A01	14880.40	14622.93	-1.73	0
Pass 5 Quads				
MQA8R01	36259.70	39785.19	9.72	0
MQA8R02	-54243.20	-55338.63	2.02	0
MQA8R03	41254.40	40536.66	-1.74	0
MQA8R04A	-46787.90	-54659.73	16.82	0
MQA8R04B	-46787.90	-54659.73	16.82	0
MQA8R05A	34185.00	31615.29	-7.52	0
MQA8R05B	34185.00	31615.29	-7.52	0
MQA8R06	6478.97	8802.69	35.87	0
MQA8R07	-46683.90	-40099.65	-14.10	0
MQA9S04	-0.00	89.30	NA	0
MQA9S05	-13752.60	-13644.63	-0.79	0
MQA9S06	19500.00	19597.92	0.50	0
MQA9S07	-19500.00	-19204.47	-1.52	0
MQA9S08	23454.80	23818.73	1.55	0
MQC9E01	-17098.50	-16716.23	-2.24	0
MQC9E02	17098.50	16716.23	-2.24	0
MQC9E03	-15928.60	-15572.42	-2.24	0
MQA9A01	22513.60	22436.20	-0.34	0

QUAD	Existing BDL	New BDL	% Change	Maxed out?
All Vertical Dispersion Quads				
MQC2R08	-15799.90	-15808.00	0.05	0
MQC2R09	15206.50	15204.29	-0.01	0
MQB2R10	-7609.16	-7345.80	-3.46	0
MQU3S01	-13430.10	-13434.56	0.03	0
MQU3S02	15605.60	15610.75	0.03	0
MQU3S03	-19094.10	-19100.30	0.03	0
MQA4R08	-31963.00	-31970.97	0.02	0
MQA4R09	23088.20	23061.16	-0.12	0
MQA4R10	-15736.10	-15320.19	-2.64	0
MQA5S01	-15073.30	-16792.74	11.41	0
MQA5S02	26901.00	26906.28	0.02	0
MQA5S03	-35965.40	-35971.59	0.02	0
MQA6R08	-51956.50	-51964.83	0.02	0
MQA6R09	39486.40	39492.81	0.02	0
MQA6R10	-21158.10	-21161.64	0.02	0
MQA7S01	-26528.20	-26533.53	0.02	0
MQA7S02	37197.50	37275.33	0.21	0
MQA7S03	-40694.20	-40694.64	0.00	0
MQA8R08	-53840.50	-53846.85	0.01	0
MQA8R09	48683.60	49551.99	1.78	0
MQA8R10	-34026.30	-36378.99	6.91	0
MQA9S02	-12426.50	-12370.26	-0.45	0
MQA9S03	20450.90	20363.42	-0.43	0

Acknowledgment

The following people are acknowledged for contributing to this task:

Arne Freyberger, Mike Spata and Mike Tiefenback for carrying out the implementation of the 12 GeV optics, followed by standard ORFP and beam qualification procedures (Quad scan etc.).

Arne Freyberger for locating time windows of usable data.

Yves Roblin for re-generating optical models corresponding to final tuned machine.

Yves Roblin and Mike Tiefenback for providing Raytrace pictures confirming implemented optics.

References

[1]. Improved Optimization of North Linac Momentum Profile for CEBAF 12 GeV Upgrade, Y. Chao, JLAB-TN-05-004
[2]. Detail of the optimization process can be found in http://www.jlab.org/~chao/Optimized_Optics.pdf.
[3]. Detail of analysis of reduction in optical sensitivity through lock correctors can be found in http://www.jlab.org/~chao/Summary_Lock_Noise.pdf.